Proceedings of the International Conference on Heat Exchanger Fouling and Cleaning - 2024 (Peer-reviewed)
April 21–26, 2024, Lisbon, Portugal; Editors: H.U. Zettler and E.M. Ishiyama

CRYSTALLIZATION FOULING ON POLYMER COMPOSITE HEAT EXCHANGER TUBES AND THE EFFECTS OF SURFACE TREATMENTS

J.-H. Imholze and *H. Glade
University of Bremen, Engineering Thermodynamics, Badgasteiner Str. 1, 28359 Bremen, Germany,
email: heike.glade@uni-bremen.de

ABSTRACT

Polymer composite materials with enhanced thermal conductivity are an attractive alternative to metal heat exchanger materials, especially in corrosive environments. Although there is increasing interest in polymer materials for heat exchangers, fouling data for polymer surfaces are very limited. In the present study, crystallization fouling on polymer composite tubes with enhanced thermal conductivity based on polypropylene or polyphenylene sulfide filled with graphite was investigated and compared with conventional metal tubes made of aluminum brass and stainless steel in a horizontal tube falling film evaporator using artificial seawater. The hydrophobic surface of the polymers leads to lower wettability and reduced heat transfer performance in heat exchangers with falling films. To increase the wettability with water, different surface treatments such as flame treatment and aluminum oxide coating were applied and their effects on crystallization fouling were investigated. The heat flux and the surface temperature were varied to compare polymer composite and metal tubes at the same conditions. The flame-treated polymer composite tubes show a lower fouling propensity than the metal tubes in terms of lower scale mass and smaller scale layer thickness, which was measured with an optical micrometer. The results suggest that the adhesive strength between deposit and substrate is lower for the polymer surfaces than for the metal surfaces. However, the polymer surface treatments have a notable influence on the fouling propensity. The results can contribute to a beneficial use of polymer composite materials in heat exchangers.

INTRODUCTION

Polymer composite materials are an attractive alternative to metals for the construction of heat exchangers, especially when corrosive fluids are being used. Polymer materials are characterized by their high corrosion and chemical resistance, low weight and great freedom in shaping. In addition, many polymers are available at a lower material price and are subject to lower price fluctuations than highly corrosion-resistant metals such as titanium, duplex stainless steels or copper-nickel alloys [1].

Unfilled polymers have been used in heat transfer applications for years but their field of application is very limited due to their poor thermal and mechanical properties [1]. To overcome these drawbacks, highly thermally conductive fillers can be inserted into the polymer matrix to get enhanced thermal performance [2]. Polymer composite tubes with enhanced thermal conductivities produced by extrusion offer benefits in many fields of heat transfer applications [3], e.g., in seawater desalination and concentration of high-salinity brines using robust and reliable falling film evaporators.

Crystallization fouling of inversely soluble salts on heat transfer surfaces, also referred to as scaling, is a major problem in evaporators with aqueous salt solutions. Scale formation leads to an additional heat transfer resistance, which deteriorates the thermal evaporator performance. Over-sizing the heat transfer area, fouling mitigation measures, cleaning methods as well as production losses during plant shutdown for cleaning result in considerable capital, operating and maintenance costs [4].

The hydrophobic surface of the polymers leads to lower wettability and consequently to reduced heat transfer performance in heat exchangers with falling films. A surface treatment must be applied to increase the wettability of the tubes with the aqueous solution without increasing the crystallization fouling propensity. Crystallization fouling has been extensively studied on metal surfaces [4,5]. Although there is a growing interest in polymer materials for heat exchangers, fouling data for polymer surfaces are very limited. The effects of polymer surface treatments on crystallization fouling have been scarcely investigated.

Solution composition, operating parameters, and heat transfer surface characteristics notably influence crystallization fouling [6]. The effects of surface characteristics on fouling, such as surface roughness and surface free energy, have been studied by several researchers [7,8]. There are contrary reports on the fouling propensity of polymer surfaces. Some reports [9,10] showed that the fouling propensity of polymer surfaces is higher than or the same as that of metal surfaces. Various studies [3, 11-13], however, indicated that polymer surfaces are less prone to fouling compared to metal surfaces. Recently, Ataki et al. [12] found that the calcium carbonate fouling affinity of polyether ether ketone (PEEK) surfaces was low compared to that of stainless steel in a flow channel test rig and the PEEK surfaces were easier to clean. The PEEK

ISBN: 978-0-9984188-3-4; Published online www.heatexchanger-fouling.com

films also showed a self-cleaning effect at high flow velocities, which was not observed on stainless steel.

In a previous study, Glade et al. [3] compared crystallization fouling on polypropylene/graphite and polyphenylene sulfide/graphite composite tubes with that on metal tubes in a stirred vessel test rig and in a horizontal tube falling film evaporator using $CaSO_4$ solution and artificial seawater, respectively. Schilling et al. [11] compared the composite tubes with metal tubes in a stirred vessel and in a falling film test rig using $CaSO_4$ and mixed $CaCO_3$ and $CaSO_4$ solutions. Both studies showed a lower fouling propensity of the polymer composite tubes compared to that of common metal tubes.

The objectives of this study are to gain a better understanding of crystallization fouling on polymer composite tubes with enhanced thermal conductivity and different surface treatments and to compare the fouling propensity of the composite tubes with that of common metal tubes in a horizontal tube falling film evaporator for seawater desalination under evaporation conditions close to those in industrial evaporators. Special focus is placed on the effects of the heat flux and the surface temperature on crystallization fouling when comparing polymer composite and metal tubes.

EXPERIMENTAL

In the following, the test rig, the tube materials and their surface characteristics, the test procedure and the scale layer analysis are described.

Test rig

The experimental study on crystallization fouling was performed in a falling film evaporator test rig at pilot plant scale, as shown in Fig. 1.

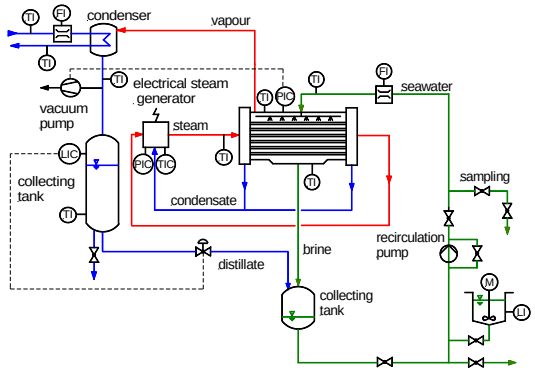

Fig. 1. Flow diagram of the falling film evaporator test rig.

The main component of the test rig is an evaporator equipped with a bank of six horizontal tubes arranged below each other. The tubes are sealed by means of O-rings and can be removed from the tube sheets. The tube length wetted by seawater amounts to 453 mm. The vertical distance between the tube centers is 50 mm. Seawater is evenly distributed onto the first tube by a toothed overflow weir and trickles down by gravity to the lower tubes, forming a thin film flow. Inspection glasses on both sides of the evaporator shell allow a visual observation of the falling film flow.

Saturated steam provided by an electrical steam generator is introduced into the tubes and condensed under vacuum conditions. The condensate flows back to the steam generator for reuse. Heat is transferred from the steam inside the tubes to the seawater on the outside of the tubes. The seawater forms a thin film on the outer tube surface. It is preheated up to saturation temperature on the first tube and then partially evaporates on the subsequent tubes. Evaporation takes place at a pressure below ambient pressure, which is maintained by a vacuum pump. The generated vapor is directed to a condenser and the condensate is collected in a tank equipped with a level indicator. After leaving the evaporator, the concentrated seawater flows into a collecting tank where it is mixed with the distillate in order to keep the salinity of the seawater approximately constant. The seawater is conveyed back to the evaporator by a centrifugal pump.

Tube materials

Experiments were carried out with polymer composite tubes and for comparison with common metal tubes. Polymer composite tubes based on polypropylene or polyphenylene sulfide filled with graphite flakes with a filler content of 50 vol%, in the following referred to as PP-GR and PPS-GR respectively, were investigated. The PP-GR tubes can be used up to a maximum temperature of 100 °C and the PPS-GR tubes can be applied up to 240 °C depending on the mechanical load. Compared to PPS-GR, the PP-based composite exhibits a slightly higher thermal conductivity, as stated in Table 1, and it is a more cost-effective solution for low-temperature heat exchangers such as falling film evaporators for seawater desalination. The composite tubes were developed and supplied by Technoform Heat Transfer Solutions (Germany). Stainless steel 1.4404, referred to as 316L, and aluminum brass (CW702R), referred to as Al brass, which are common evaporator tubing materials, were used for comparison. Tube data are summarized in Table 1.

Table 1. Tube data (wetted tube length L = 453 mm).

Tube material	Thermal conductivity in radial direction / W/(m K)	Tube outside diameter / mm	Tube wall thickness / mm
PP-GR	6.5 (25 °C) 5.3 (100 °C)	24	1.5
PPS-GR	4.5 (25 °C) 4.3 (100 °C)	24	1.5
316L	15 (20 °C) 16 (100 °C)	24	1
Al brass	100 (20 °C) 112 (100 °C)	25	1

ISBN: 978-0-9984188-3-4; Published online www.heatexchanger-fouling.com

The major disadvantage of unfilled polymers for using them in heat transfer applications is their very low thermal conductivity between 0.1 and 0.5 W/(m K) [2]. The high graphite content of the composite tubes leads to their anisotropic thermal conductivity. The application of composite tubes in heat exchangers requires a high thermal conductivity in radial direction (through the tube wall). The thermal conductivities of the PP-GR and PPS-GR tubes were determined in radial direction using a laser flash analysis instrument (LFA 457 MicroFlash, Netzsch-Gerätebau GmbH, Germany). As shown in Table 1, the polymer composite tubes have a remarkably high thermal conductivity in the radial direction. The through-wall thermal conductivity of the tubes made of polypropylene filled with 50 vol% graphite is increased by a factor of 30 compared to pure polypropylene, resulting in a thermal conductivity of 6.5 W/(m K) at 25 °C.

In falling film evaporators, the entire tube surface must be covered with a thin liquid film and film break-down must be avoided to ensure decent heat transfer performance and lower the risk of severe crystallization fouling starting at the edges of the dry patches. To increase the wettability of the polymer surfaces, different surface treatments, namely flame treatment and aluminum oxide coating, were applied on the outside of the tubes and their effects on fouling were studied. Flame treatment is a common technique for improving the surface properties of polymers [14]. Therefore, the PP-GR and PPS-GR tubes were flame treated (referred to as flame trd.) prior to each experiment. Moreover, aluminum oxide (Al_2O_3) coating, which is inert to acids and alkalis, was investigated. Spray coating, using a mass flow rate of 80 g/min, was applied to the PP-GR tubes (referred to as PP-GR Al_2O_3).

The advancing contact angles were measured on top of the composite and metal tubes using a drop shape analysis instrument (OCA 50, DataPhysics Instruments GmbH, Germany). The surface free energy was determined on the basis of the contact angle measurements with three test liquids (water, diiodomethane and ethylene glycol) and Young's equation. The solid/liquid interfacial free energy between tube surface and droplet in Young's equation was calculated using the geometric mean approach. Contact angles were measured three times on each tube. Table 2 shows the contact angles with water and the surface free energies.

The untreated PP-GR and PPS-GR tubes exhibit contact angles with water higher than 90° and the surface free energy of PP-GR is lower than the one of PPS-GR. The relatively low polar component of the surface free energy of the untreated PP-GR and PPS-GR tubes results in their hydrophobic behavior. In comparison, the Al brass and 316L tubes show lower contact angles of about 72° and 65°, respectively, and a relatively high polar component of the surface free energy.

Table 2. Contact angles and surface free energies (dispersive (d) and polar (p) components of surface free energy) of the tube materials.

Tube material	Surface energy (total) / mJ/m²	Surface energy (d) / mJ/m²	Surface energy (p) / mJ/m²	Contact angle with water / °
PP-GR	29.47 ± 0.55	27.45 ± 1.34	2.03 ± 1.10	92.54 ± 4.94
PP-GR flame trd.	42.65 ± 1.96	29.58 ± 0.55	13.08 ± 2.18	63.32 ± 0.55
PP-GR Al_2O_3	19.86 ± 0.72	17.56 ± 0.40	2.30 ± 0.83	135.16 ± 4.65
PPS-GR	40.73 ± 1.70	39.93 ± 2.03	0.80 ± 0.97	91.87 ± 7.06
PPS-GR flame trd.	60.32 ± 0.78	35.22 ± 0.55	25.10 ± 0.78	34.24 ± 0.55
316L	40.49 ± 1.42	28.75 ± 0.82	11.74 ± 0.65	64.83 ± 1.93
Al brass	36.83 ± 0.16	27.94 ± 1.34	8.89 ± 1.19	71.58 ± 1.79

As shown in Table 2, flame treatment reduces the contact angle for PP-GR to 63° and for PPS-GR to 34° and increases the polar component which results in a hydrophilic surface. Very high contact angles were measured on the Al_2O_3-coated tubes due to their high surface roughness leading to measuring difficulties. Wenzel [15] stated that rough surfaces can increase the hydrophobic or hydrophilic behavior, respectively.

Surface roughness parameters were measured at twelve positions along and around the tubes using a tactile stylus unit (MarSurf GD25, Mahr GmbH, Germany). Table 3 summarizes the mean roughness *Ra* and the roughness depth *Rz*.

Table 3. Surface roughness of the tube materials.

Tube material	Mean roughness *Ra* / µm	Roughness depth *Rz* / µm
PP-GR	0.37 ± 0.06	2.37 ± 0.52
PP-GR flame trd.	0.37 ± 0.05	2.38 ± 0.34
PP-GR Al_2O_3	3.47 ± 0.82	21.35 ± 4.55
PPS-GR	2.01 ± 0.52	14.43 ± 3.90
PPS-GR flame trd.	2.01 ± 0.51	15.15 ± 3.94
PPS-GR smooth	0.45 ± 0.07	2.52 ± 0.31
316L	0.42 ± 0.03	3.66 ± 0.31
Al brass	0.62 ± 0.22	4.40 ± 1.21

The PP-GR tubes exhibit the lowest roughness parameters. Compared to PP-GR, the higher viscosity of the PPS-GR compound poses a greater challenge during tube extrusion. Both PPS-GR tubes with notably higher roughness and advanced PPS-GR tubes with a smooth surface (referred to as PPS-GR smooth) were tested. The advanced smooth PPS-GR tubes and the 316L tubes have roughness parameters similar to the PP-GR tubes whereas the roughness depth of the 316L tubes is slightly higher. The roughness parameters of the Al brass tubes are slightly higher but still in the same order of magnitude. The flame treatment of the polymer

ISBN: 978-0-9984188-3-4; Published online www.heatexchanger-fouling.com

surfaces does not notably affect their roughness. However, the PP-GR tubes with Al_2O_3 coating have a significantly rougher surface.

Test procedure

New tubes were used for each experiment. The PP-GR and PPS-GR tubes were cleaned with pressurized air prior to the application of the flame treatment. The 316L and Al brass tubes were thoroughly cleaned with deionized water, isopropyl alcohol and acetone.

Artificial seawater with a high salinity of 65 g/kg and an ionic strength of 1.39 mol/kg was used for the experiments, representing concentrated brine. The initial pH value was approximately 8.3. The formulation of the artificial seawater originates from oceanography [16], including 99.9 mass% of salts in natural seawater. Experiments with 240 L of artificial seawater and time periods of 50 h were found to be favorable. The time period is long enough to find differences in crystallization fouling and the supersaturation level is still high enough.

A wetting rate, which is the mass flow rate per unit tube length, of Γ = 0.14 kg/(s m) was chosen for the top tube in order to ensure complete tube wetting. Crystallization fouling on PP-GR flame trd., PP-GR Al_2O_3, PPS-GR flame trd., PPS-GR smooth flame trd., 316L and Al brass tubes was studied at an evaporation temperature of 65 °C and a condensation temperature of 70 °C. For a better comparison of the composite and metal tubes having different thermal conductivities and wall thicknesses, the effects of heat flux and surface temperature were studied using PP-GR flame trd. tubes by varying the condensation temperature between 68 °C and 74 °C, while keeping the evaporation temperature constant at 65 °C.

During the test runs, temperatures, pressures and volume flow rates were measured (see Fig. 1). Distillate was collected at regular intervals and the distillate volume flow rate was measured. On the basis of the measured data, the average overall heat transfer coefficient was determined using energy balances and overall heat transfer equations. Furthermore, the heat transfer coefficient during condensation inside the horizontal tubes was calculated [17]. Fig. 2 shows the calculated heat flux and the outside wall temperature for the PP-GR, 316L and Al brass tubes depending on the temperature difference.

In order to avoid nucleate boiling and to ensure that vapor is formed only on the film surface, the difference between wall temperature and saturation temperature must not be too large. In falling film evaporators with vertical tubes, it should not exceed 6 K for water [18]. Arzt [19] found that surface evaporation of water films prevails for heat fluxes lower than 30 kW/m² in horizontal tube falling film evaporators. As only low temperature differences and heat fluxes were applied during the test runs (see Fig. 2), vapor was mainly formed on the film surface without notable formation of vapor bubbles, what was confirmed by visual observation.

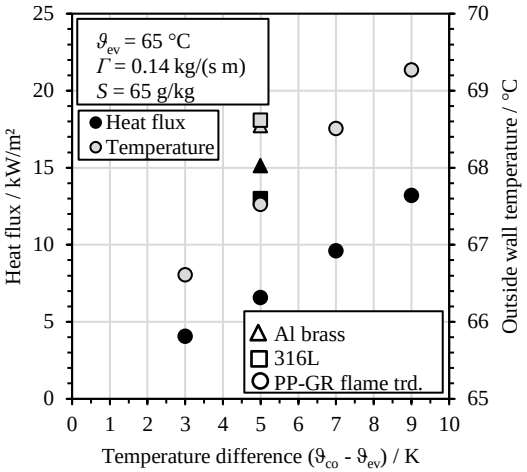

Fig. 2. Heat flux and outside wall temperature depending on the temperature difference between condensation and evaporation side for PP-GR flame trd., 316L and Al brass tubes.

The inside of the evaporator was manually cleaned with deionized water and with diluted acetic acid solution after each test. The collecting tank for the seawater was cleaned with water jets and the whole circuit was cleaned by flushing with deionized water for minimum three days.

Scale layer analysis

In order to analyze only the scale on the main tube body, the scale at the edges was removed over a length of 10 mm on each side.

A new method has been developed to measure the scale layer thickness using a high-resolution optical micrometer (optoCONTROL 2600, Micro-Epsilon Messtechnik GmbH & Co. KG, Germany). The micrometer uses light-emitting diode (LED) technique and exhibits a resolution of 0.1 µm, a reproducibility of ± 1 µm and a linearity of max. ± 3 µm [20]. As depicted in Fig. 3, the diameter of the tube with the adherent scale layer and the diameter of the tube after dissolving the scale in acetic acid were measured. Measurements were taken at four circumferential angles, namely 0°, 45°, 90° and 135°, and at 25 positions in axial direction.

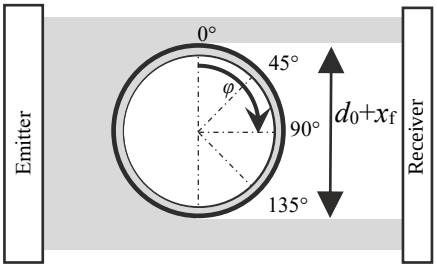

Fig. 3. Illustration of the measurement of the scale layer thickness x_f using the LED micrometer.

ISBN: 978-0-9984188-3-4; Published online www.heatexchanger-fouling.com

The third, fourth and fifth tube with adherent scale was immersed in a 10 mass% acetic acid solution at 42 °C for 2 h in order to dissolve the scale. The concentrations of calcium, magnesium, sulfur and strontium in the solution were determined using inductively coupled plasma optical emission spectroscopy (ICP-OES). The scale on the sixth tube was analyzed using scanning electron microscopy (SEM) in combination with energy dispersive X-ray analysis (EDX), X-ray diffraction (XRD) and Fourier-transform infrared with attenuated total reflection (FTIR-ATR).

RESULTS

The fouling propensity of the polymer composite tubes with different surface characteristics was studied and compared to 316L and Al brass tubes at an evaporation temperature of 65 °C and a condensation temperature of 70 °C. The experimental results are presented in the following.

Fig. 4 shows SEM images of the scale on tube No. 6 for the various materials.

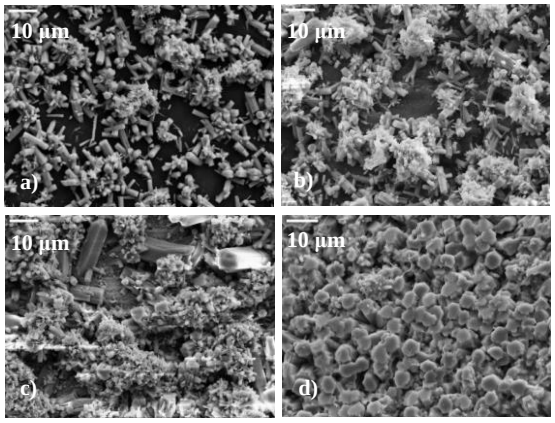

Fig. 4. SEM images of a) PP-GR flame trd., b) PPS-GR flame trd., c) 316L, d) Al brass tube No. 6 (seawater, S = 65 g/kg, ϑ_{co} = 70 °C, ϑ_{ev} = 65 °C, Γ = 0.14 kg/(s m), t = 50 h).

The surface of the flame-treated PP-GR tube was only weakly covered with scale after 50 hours, as shown in Fig. 4a). Mainly $CaCO_3$ crystals and a mix of Ca-, Mg-, S- and Sr-containing scale were detected. Many spots on the tube surface were uncovered. As shown in Fig. 4b), the flame-treated PPS-GR tube was more covered with scale than the flame-treated PP-GR tube. Mainly $CaCO_3$ crystals but also some $CaSO_4$ were detected on the tube surface. Moreover, Mg and Sr were identified. The SEM image in Fig. 4c) shows a dense scale layer on the 316L tube surface which contains $CaCO_3$, $CaSO_4$ and Mg- and Sr-containing scale. As shown in Fig. 4d), the Al brass tube is completely covered with a dense scale layer of $CaCO_3$ and some Mg-containing scale. Further SEM images also show $CaSO_4$ and Sr-containing scale on the Al brass tube.

On each tube surface, the calcium mass was considerably higher than the magnesium, sulfur and strontium masses measured by means of ICP-OES. Figs. 5 and 6 show the calcium and the magnesium masses per unit tube surface area, respectively. Mainly $CaCO_3$ precipitated on the tube surfaces and the $CaCO_3$ scale increased from the third to the fifth tube. The calcium and magnesium masses on the flame-treated PP-GR and PPS-GR tubes were considerably lower than those on the 316L and Al brass tubes. Similarly low calcium and magnesium masses were deposited on the flame-treated smooth PPS-GR tubes as on the flame-treated PP-GR tubes. However, calcium and magnesium masses on the flame-treated rough PPS-GR tubes were higher than those on the flame-treated smooth PPS-GR tubes. On the Al_2O_3-coated PP-GR tubes, the calcium mass was significantly higher than that on the flame-treated PP-GR and PPS-GR tubes and the magnesium mass was higher than that on the flame-treated PP-GR and smooth PPS-GR tubes.

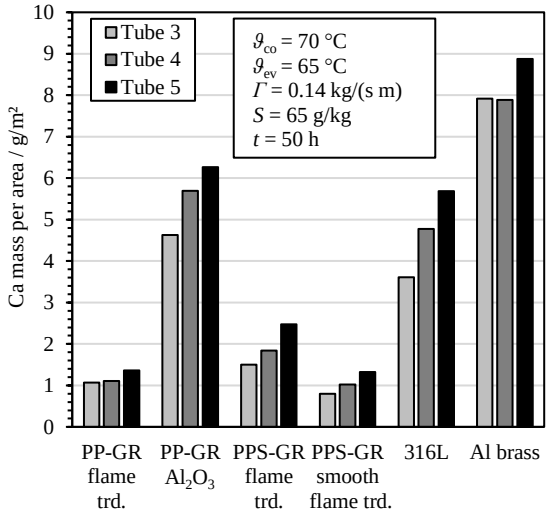

Fig. 5. Calcium mass per unit surface area on surface-treated polymer composite and metal tubes.

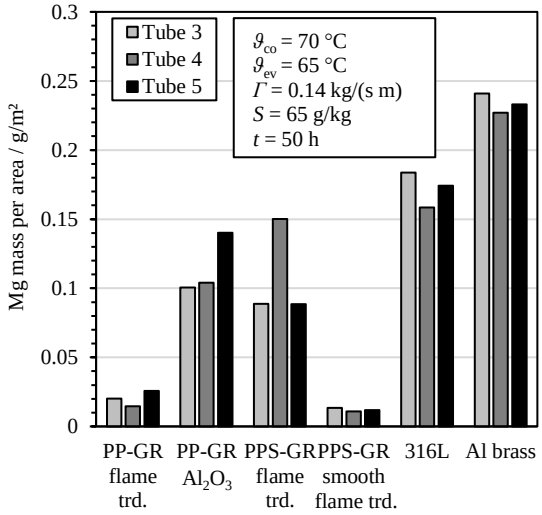

Fig. 6. Magnesium mass per unit surface area on surface-treated polymer composite and metal tubes.

ISBN: 978-0-9984188-3-4; Published online www.heatexchanger-fouling.com

The scale layer thickness was measured on the polymer composite and metal tubes using the LED micrometer. Fig. 7 shows the results for the fifth tube at different circumferential angles.

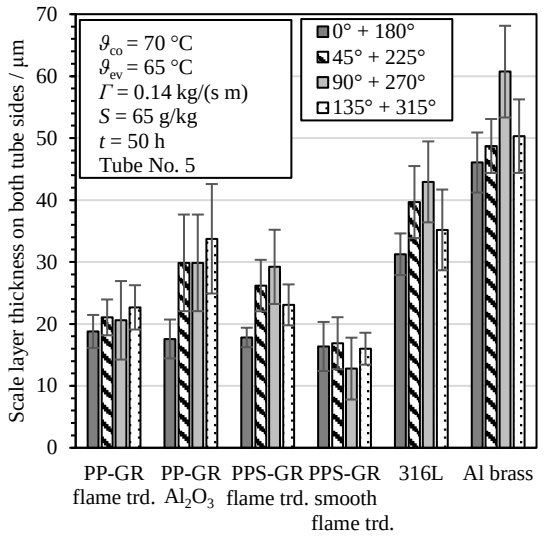

Fig. 7. Scale layer thickness on both sides of tube No. 5 of surface-treated composite and metal tubes.

As shown in Fig. 7, the scale layer thicknesses on the flame-treated PP-GR and flame-treated smooth PPS-GR tubes were considerably lower than those on the 316L and Al brass tubes. The scale layers at different circumferential angles of the Al brass tube were about 2 to 5 times thicker than those on the flame-treated PP-GR and flame-treated smooth PPS-GR tubes. The scale thicknesses on the Al_2O_3-coated PP-GR and flame-treated rough PPS-GR tubes were similar and higher than those on the flame-treated PP-GR and smooth PPS-GR tubes. The thickest scale layer on tube No. 3, 4 and 5 of both metals was measured on the tube sides (90° and 270°), as shown in Fig. 7 for tube No. 5. However, this was not the case for the polymer composite tubes.

As the composite and metal tubes have different thermal conductivities and wall thicknesses, the effects of heat flux and surface temperature on scale formation were studied using flame-treated PP-GR tubes by varying the condensation temperature between 68 °C and 74 °C, while keeping the evaporation temperature constant at 65 °C, as shown in Fig. 2. The calcium and magnesium masses per area on PP-GR flame trd., 316L and Al brass tubes for varying heat fluxes are shown in Fig. 8. The calcium masses on the flame-treated PP-GR tubes increase with rising heat flux. However, the calcium masses are significantly lower compared to those on 316L and Al brass tubes at similar heat flux and surface temperature (see Fig. 2).

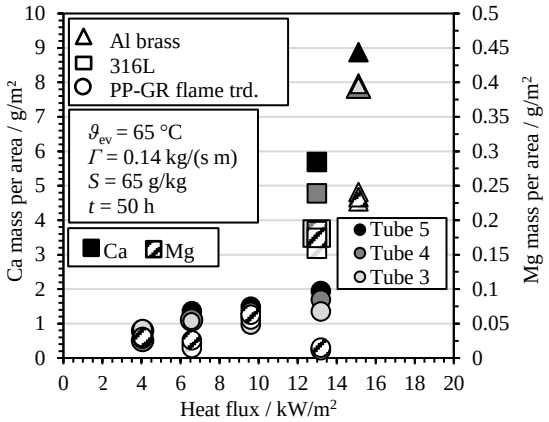

Fig. 8. Calcium and magnesium masses per area on PP-GR flame trd., 316L and Al brass tubes for varying heat fluxes.

DISCUSSION

Both on polymer composite and on metal tubes, mixed scale formed in contact with concentrated seawater in the falling film evaporator. The composition of the scale on the polymer composite and metal tubes is similar. The scale on all tube materials mainly consists of calcium carbonate in the form of aragonite, which was detected by XRD and FTIR-ATR and can be seen in the SEM images in Fig. 4. Calcium sulfate crystals (gypsum) formed on some spots during falling film evaporation which can be explained by locally high concentrations in the evaporating thin liquid film. The magnesium-containing scale mass on each tube is significantly lower than the calcium scale mass.

Scale formation is dominated by calcium carbonate and magnesium hydroxide precipitation during seawater evaporation in falling film evaporators [5,21,22]. Krömer et al. [21] and Stärk et al. [5] demonstrated in fouling experiments with artificial seawater that the surface of metal tubes was covered with a two-layer scale comprising a thin, flaky, magnesium-rich base layer underneath a thick layer of calcium carbonate crystals in the form of aragonite. X-ray diffraction mainly indicated magnesium hydroxide (brucite) or iowaite in the magnesium-containing scale. A shift of pH to high values in the seawater film due to CO_2 release and, additionally, cathodic reactions on the metal surface resulting in a locally enhanced OH^- concentration may promote a high degree of supersaturation of $Mg(OH)_2$ to drive its precipitation on the tube surface. Thus, the deposition of magnesium-containing scale might be different on polymer surfaces than on metal surfaces. A thin layer of flaky $Mg(OH)_2$ crystals on the tube surface has not been observed on the polymer surfaces so far. The magnesium-containing scale was mainly found on the carbonate crystals.

However, there is a significant difference in the scale quantity on polymer composite and metal tubes. The $CaCO_3$ scale mass and the scale layer

ISBN: 978-0-9984188-3-4; Published online www.heatexchanger-fouling.com

thickness are significantly lower on flame-treated PP-GR and PPS-GR tubes than on 316L and Al brass tubes, as shown in Figs. 5 and 7. The SEM images in Fig. 4 show many uncovered spots on the PP-GR and PPS-GR surfaces, whereas a very dense scale layer formed on the Al brass tubes.

The higher scale mass on Al brass compared to that on stainless steel 316L tubes can be explained by the slightly higher surface roughness and the presence of corrosion products on the copper alloy as well as by the higher heat flux. A higher scale mass on Al brass tubes compared to that on duplex stainless steel was also found by Glade et al. [3].
Scale formation increased from tube No. 3 to tube No. 5 for each tube material. It can be explained by the evaporation of water which increases the salt concentrations and, thus, the supersaturation.

Increased scale formation on the rougher PPS-GR tubes compared to the advanced smoother PPS-GR tubes can be explained by the effect of surface roughness on crystallization fouling. The significantly higher $CaCO_3$ masses on the PP-GR tubes with Al_2O_3 coating compared to the flame-treated PP-GR tubes can also be attributed to the increased surface roughness. It is believed that surface roughness enhances nucleation and increases the contact surface area which in turn increases adhesion [4,7].

As shown in Fig. 8, the $CaCO_3$ masses on flame-treated PP-GR tubes increase with rising heat flux, because the evaporation rate increases and, thus, the salt concentrations and the supersaturation rise. Furthermore, the heat flux considerably affects the strength of deposits by influencing the number of active nucleation sites [6]. However, the $CaCO_3$ mass on the PP-GR tubes is significantly lower than that on metal tubes at similar heat flux and surface temperature, as shown in Fig. 8. These results demonstrate that the differences in crystallization fouling between the polymer composite tubes and the metal tubes can be mainly attributed to their surface characteristics.

As shown in Table 2, flame treatment of the PP-GR and PPS-GR surfaces increases the surface free energy, especially the polar part, and, thus, the wettability of the surfaces with water. However, comparing the surface free energies of the materials and their fouling propensity shows that there is no simple correlation between surface free energy and fouling behavior. A correlation cannot be based only on the surface properties of the heat transfer surface [7]. The adjacent crystalline deposit has to be taken into account because it also influences molecular interaction at the interface crystal/heat transfer surface. Furthermore, the co-precipitation of calcium- and magnesium-containing salts makes it even more complicated. It is conceivable that some metals promote the formation of magnesium-containing scale which in turn influences the precipitation of $CaCO_3$ scale. The interfacial interactions between the tube surface and $Mg(OH)_2$ crystals and the interactions between $Mg(OH)_2$ and $CaCO_3$ crystals should be taken into account [5].

Since it was observed that the scale layer can be detached more easily from the flame-treated PP-GR and PPS-GR tubes than from the Al_2O_3-coated PP-GR and metal tubes, it is assumed that the adhesive force between scale layer and substrate is lower for the flame-treated composite tubes, which would increase the removal rate relative to the rate of deposition. It is often assumed that the adhesive force between the deposit and the substrate is lower for polymer surfaces than for metal surfaces [12].

The scale layer thickness measurements at different circumferential angles of the tubes also indicate differences between polymer composite and metal tubes. Waack et al. [22] measured the liquid film thickness with an optical micrometer and correlated it with scale formation on metal tubes. The strongest scale formation occurred at the sides of the tubes (90° and 270°) followed by the tube top. Least scale formed on the tube bottom. Assuming diffusion-controlled $CaCO_3$ crystallization in the laminar-wavy falling film, the thin liquid film at the tube sides leads to a small mass transfer resistance and to increased scale formation on metal tubes.

In the present study, the thickest scale layer on the 316L and Al brass tubes was measured on the tube sides, which is consistent with the results of Waack et al. [22]. In contrast, the thickest scale layer on the composite tubes was not found on the tube sides in all cases, as shown in Fig. 7. These results can also be explained by different adhesion forces between the deposit and the tube materials. A lower adhesion force between the deposit and the polymer surface compared to metals can lead to higher scale removal rates, especially on the tube sides (90° and 270°) caused by the higher flow velocity.

CONCLUSIONS

In the present study, crystallization fouling on polymer composite tubes with enhanced thermal conductivity based on polypropylene or polyphenylene sulfide filled with graphite was investigated and compared with aluminum brass and stainless steel 316L tubes in a horizontal tube falling film evaporator using artificial seawater. To increase the wettability of the polymer surfaces with water, flame treatment and aluminum oxide coating were applied and their effects on fouling were studied. A novel method has been developed to measure the scale layer thickness using a high-resolution optical micrometer.

The results demonstrate that the flame-treated polymer composite tubes exhibit a considerably lower crystallization fouling propensity than the metal tubes in terms of lower scale mass and smaller scale layer thickness. The $CaCO_3$ masses on flame-treated polymer composite tubes increase with rising heat flux. However, the $CaCO_3$ masses on the flame-

ISBN: 978-0-9984188-3-4; Published online www.heatexchanger-fouling.com

treated composite tubes are significantly lower than those on the metal tubes at similar heat flux and surface temperature. These results show that the differences in scale formation between the polymer composite tubes and the metal tubes can be mainly attributed to their surface characteristics. However, there is no simple correlation between surface free energy and fouling behavior. It appears that the adhesive force between deposit and substrate is lower for polymer surfaces than for metal surfaces.

In future work, the adhesion between the deposit and the polymer surface or the metal surface, respectively, should be studied in more detail. The results can contribute to a better understanding of fouling on polymer surfaces and to a beneficial use of polymer composite materials in heat exchangers.

ACKNOWLEDGEMENTS

The authors would like to thank Technoform Heat Transfer Solutions (Germany) for supplying the polymer composite tubes.

The study is part of a project which has received funding from the European Union's Horizon 2020 research and innovation programme under grant agreement No. 869703.

NOMENCLATURE

d_o	Outside tube diameter, mm
L	Tube length, mm
Ra	Mean roughness, µm
Rz	Roughness depth, µm
S	Salinity, g/kg
t	Time, h
x_f	Scale layer thickness on both tube sides, µm
Γ	Wetting rate, kg/(s m)
ϑ	Temperature, °C
φ	Circumferential angle, °

Subscript

co	Condensation
ev	Evaporation

REFERENCES

[1] Cevallos, J. G., Bergles, A. E., Bar-Cohen, A., Rodgers, P., and Gupta, S. K., Polymer Heat Exchangers - History, Opportunities, and Challenges, *Heat Transfer Engineering*, vol. 33, no. 13, pp. 1075–1093, 2012.

[2] Chen, H., Ginzburg, V. V., Yang, J., Yang, Y., Liu, W., Huang, Y., Du, L., and Chen, B., Thermal conductivity of polymer-based composites: fundamentals and applications, *Progress in Polymer Science*, vol. 59, pp. 41–85, 2016.

[3] Glade, H., Moses, D., and Orth, T., Polymer Composite Heat Exchangers, in *Innovative Heat Exchangers*, eds. H.-J. Bart and S. Scholl, pp. 53–116, Springer International Publishing, Cham, 2018.

[4] Müller-Steinhagen, H., C4 Fouling of Heat Exchanger Surfaces, in *VDI Heat Atlas*, ed. VDI, pp. 79–104, Springer Berlin, Heidelberg, 2010.

[5] Stärk, A., Krömer, K., Loisel, K., Odiot, K., Nied, S., and Glade, H., Impact of Tube Surface Properties on Crystallization Fouling in Falling Film Evaporators for Seawater Desalination, *Heat Transfer Engineering*, vol. 38, 7-8, pp. 762–774, 2017.

[6] Zhao, X., and Chen, X. D., A Critical Review of Basic Crystallography to Salt Crystallization Fouling in Heat Exchangers, *Heat Transfer Engineering*, vol. 34, 8-9, pp. 719–732, 2013.

[7] Geddert, T., Augustin, W., and Scholl, S., Induction Time in Crystallization Fouling on Heat Transfer Surfaces, *Chemical Engineering Technology*, vol. 34, no. 8, pp.1303-1310, 2011.

[8] Zettler, H. U., Wei, M., Zhao, Q., and Müller-Steinhagen, H., Influence of Surface Properties and Characteristics on Fouling in Plate Heat Exchangers, *Heat Transfer Engineering*, vol. 26, no. 2, pp. 3–17, 2005.

[9] Wu, Z., Davidson, J. H., and Francis, L. F., Effect of water chemistry on calcium carbonate deposition on metal and polymer surfaces, *Journal of Colloid and Interface Science*, vol. 343, no. 1, pp. 176–187, 2010.

[10] Sanft, P., Francis, L. F., and Davidson, J. H., Calcium Carbonate Formation on Cross-Linked Polyethylene (PEX) and Polypropylene Random Copolymer (PP-r), *Journal of Solar Energy Engineering*, vol. 128, no. 2, pp. 251–254, 2006.

[11] Schilling, S., Glade, H., and Orth, T., Investigation of Crystallization Fouling on Novel Polymer Composite Heat Exchanger Tubes, *Heat Transfer Engineering*, vol. 43, pp. 1326-1336, 2022.

[12] Ataki, A., Kiepfer, H., and Bart, H.-J., Investigations on crystallization fouling on PEEK films used as heat transfer surfaces: experimental results, *Heat and Mass Transfer*, vol. 56, no. 5, pp. 1443–1452, 2020.

[13] Kazi, S. N., Duffy, G. G., and Chen, X. D., Mineral scale formation and mitigation on metals and a polymeric heat exchanger surface, *Applied Thermal Engineering*, vol. 30, 14-15, pp. 2236–2242, 2010.

[14] Strobel, M., Branch, M. C., Ulsh, M., Kapaun, R. S., Kirk, S., and Lyons, C. S., Flame surface modification of polypropylene film, *Journal of Adhesion Science and Technology*, vol. 10, no. 6, pp. 515–539, 1996.

[15] Wenzel, R. N., Resistance of Solid Surfaces to Wetting by Water, *Industrial & Engineering Chemistry*, vol. 28, no. 8, pp. 988–994, 1936.

ISBN: 978-0-9984188-3-4; Published online www.heatexchanger-fouling.com

[16] Kester, D. R., Duedall, I. W., Connors, D. N., and Pytkowicz, R. M., Preparation of artificial seawater, *Limnology Oceanography*, vol. 12, no. 1, pp. 176–179, 1967.
[17] Chato, J. C., Laminar condensation inside horizontal and inclined tubes, *ASHRAE Journal*, vol. 4, pp. 52–60, 1962.
[18] Schnabel, F., M3 Heat Transfer to Falling Films at Vertical Surfaces, in *VDI Heat Atlas*, ed. VDI, pp. 1287–1294, Springer Berlin, Heidelberg, 2010.
[19] Arzt, B., Meerwasserentsalzung durch Mehrfach-Effekt-Stack Horizontalrohrverdampfung, Ph.D. thesis, RWTH Aachen, Germany, 1984.
[20] Micro-Epsilon Messtechnik GmbH & Co. KG, optoControl 2600 - High resolution LED micrometer, Technical data sheet, www.micro-epsilon.co.uk.
[21] Krömer, K., Will, S., Loisel, K., Nied, S., Detering, J., Kempter, A., and Glade, H., Scale Formation and Mitigation of Mixed Salts in Horizontal Tube Falling Film Evaporators for Seawater Desalination, *Heat Transfer Engineering*, vol. 36, 7-8, pp. 750–762, 2015.
[22] Waack, W., Glade, H., and Nied, S., Falling film flow characteristics on horizontal tubes and their effects on scale formation in seawater evaporators, *Desalination and Water Treatment*, vol. 211, pp. 1–14, 2021.

ISBN: 978-0-9984188-3-4; Published online www.heatexchanger-fouling.com